Observation of the $[1s2s](^{3,1}S)n\ell n'\ell'\ ^1P$ inner-shell doubly excited states of Ne by photoion yield spectroscopy

M. Oura and H. Yamaoka
SPring-8/RIKEN, Harima Institute, 1-1-1 Kouto, Mikazuki, Sayo, Hyogo 679-5148, Japan

Y. Senba and H. Ohashi
SPring-8/JASRI, 1-1-1 Kouto, Mikazuki, Sayo, Hyogo 679-5198, Japan

F. Koike
School of Medicine, Kitasato University, 1-15-1 Kitasato, Sagamihara, Kanagawa 228-8555, Japan
(Received 9 August 2004; published 13 December 2004)

The photoabsorption spectrum of Ne in the excitation energy region of the $[1s2s](^{3,1}S)n\ell n'\ell'$ doubly excited states has been measured using high brilliant soft x-ray undulator radiation, where square brackets indicate hole states. The observed absorption spectrum was analyzed with the aid of theoretical calculations based on the multiconfiguration Dirac-Fock (MCDF) method. The computation has revealed that the observed features are successfully assigned with several series of the resonant double excitations, such as the $[1s2s](^{3,1}S)3snp$ $(3\leqslant n\leqslant 6)$ and the $[1s2s](^3S)3pns$ $(4\leqslant n\leqslant 6)$ series. The $[1s2s]n\ell n'\ell'$ double excitation resonance leading to the lowest $[1s2s](^3S)3s3p$ state was analyzed using the well-known parametrized Fano profile. The energy as well as the width of the resonance for such highly correlated multiply excited state have been determined and the possible decay channels for the $[1s2s](^3S)3s3p$ state were also discussed.

DOI: 10.1103/PhysRevA.70.062502 PACS number(s): 32.70.Cs, 32.70.Fw, 32.70.Jz

I. INTRODUCTION

Weak structures originated in the resonant multielectron excitation processes are often observed in the photoabsorption spectra far above the core-ionization threshold of atoms, molecules, and solids [1–9]. Since their appearance departs from the independent particle model, detailed studies on the excitation mechanism and the relaxation dynamics for these resonant multielectron processes in combination with the sophisticated theoretical calculations will provide unique information about the electronic correlation in the initial state as well as the final ionic states [10–13].

Recently, Oura *et al.* have studied the angle-resolved resonant Auger (RA) emission from the $[1s2p](^{3,1}P)3p^2\ ^1P$ doubly excited two-particle–two-hole (hereafter referred to as $2p$-$2h$) states of Ne [14]. They proposed the existence of double-spectator type and spectator-shakeup type RA transitions with the aid of theoretical calculations, in which the kinetic energies and the transition amplitudes were calculated based on the Hartree-Fock approximation [15] and the anisotropy parameters were calculated using a pure *LS* coupling approach [16]. More recently, Oura *et al.* have also studied the spectral evolution of the double-spectator type RA transitions leading to the Ne^+ $[2p^3](^2D)3p^2\ ^2P$ and ^2F states and to the Ne^+ $[2p^3](^2P)3p^2\ ^2D$ state across the $[1s2p](^3P)3p^2\ ^1P$ double excitation resonance at 902.45 eV with fine-energy step [17]. It is revealed that the detailed observation of these double-spectator type RA transitions has elucidated their characteristics of the RA emissions [18,19] and has given us a firm support to the assignments for these RA transitions made in the previous study [14].

In this paper, we report an observation of deeply bound $[1s2s](^{3,1}S)n\ell n'\ell'\ ^1P$ inner-shell doubly excited $2p$-$2h$ states of Ne atoms probed by high-resolution photoion yield spectroscopy. Prince *et al.* [20] have recently measured the absolute photoabsorption cross section in the same energy region and observed several states above the $[1s2p]$ double ionization threshold. They assigned these new features to the $[1s2s]nsn'p$ series. Here we give much detailed assignments for these new features with the aid of accurate theoretical calculations based on the multiconfiguration Dirac-Fock (MCDF) method. Resonant doubly excited states converging to the $[1s2s](^3S)3s\epsilon p$ and $[1s2s](^3S)3p\epsilon s$ series limits are reported.

II. EXPERIMENT

The measurement was carried out using the photon-ion merged-beam apparatus [21,22] at the newly constructed soft x-ray undulator beamline BL17SU [23] at SPring-8, an 8 GeV synchrotron radiation facility in Japan. The combination of high brilliance and narrow bandpass ($E/\Delta E \sim 10\,000$) of the soft x-ray radiation from BL17SU [24,25] has allowed us to perform the high-resolution measurement on the inner-shell doubly excited states in the present energy region. Although the photon-ion merged-beam apparatus is originally aimed at performing a photoabsorption experiment on the ionic target [26–28], we utilized this apparatus for the neutral gas target in the present study. Gaseous Ne atoms were introduced into an interaction region of the apparatus, where the photoabsorption events followed by Auger processes will occur. Product ions were extracted from the interaction region and accelerated by the applied voltage V_{int} up to the kinetic energy of qV_{int} corresponding to its charge state q. Then the extracted ion beam was analyzed by an

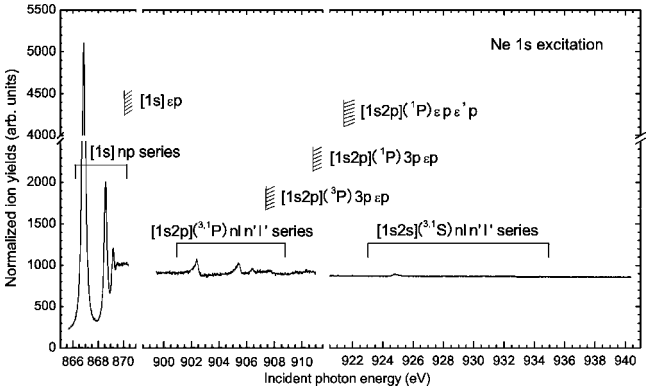

FIG. 1. Photoabsorption spectra in the Ne 1*s* excitation region measured by means of photoion yield spectroscopy. Several series limits are indicated in the figure. See text for details.

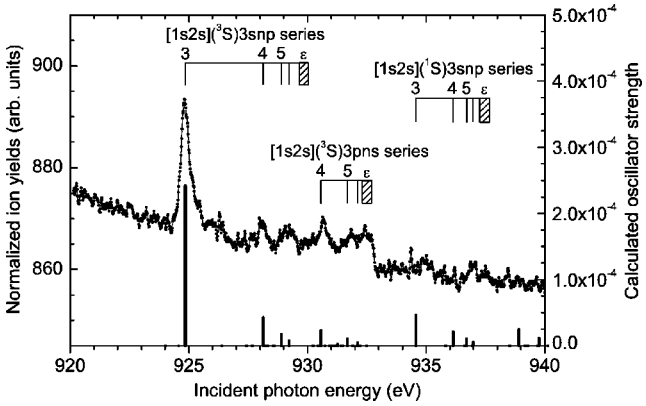

FIG. 2. Photoabsorption spectrum in the region of the $[1s2s](^{3,1}S)n\ell n'\ell'$ doubly excited 2*p*-2*h* states of Ne. The calculated oscillator strengths and the energy positions of $[1s2s](^{3,1}S)3snp$ $(3\leqslant n\leqslant 6)$ and $[1s2s](^{3}S)3pns$ $(4\leqslant n\leqslant 6)$ double excitation resonances as well as their series limits are also indicated in the figure.

electrostatic cylindrical mirror analyzer and the total intensity of the product ions was measured using an electron multiplier. Thus the apparatus was operated as a part of the PHOBIS (PHOton Beam Ion Source) [29] mode in which it enabled us to perform the photoion yield spectroscopy.

In the present study, the photon bandpass was estimated to be about 121 meV, at a photon energy of 867.12 eV, by measuring the photoion yield spectrum of Ne in the region of the $[1s]np$ $(n=3,4,\ldots,\epsilon)$ excitation. We have adopted the value of natural lifetime width 240 meV [30] of the Ne $[1s]3p$ state in the estimation of photon bandpass. The accuracy of the energy scale for the incident photon beam was estimated to be about ±0.12 eV (±0.03 eV) for absolute (relative) scale. The high-resolution photoabsorption spectrum was then measured in the region of the resonant double excitation.

III. RESULTS AND DISCUSSION

Figure 1 shows the broadband absorption spectrum in the Ne 1*s* excitation region measured by means of photoion yield spectroscopy. The spectra are categorized to three different excitation regions, i.e., the $[1s]np$ Rydberg series, the $[1s2p](^{3,1}P)n\ell n'\ell'$ double excitation region, and the $[1s2s](^{3,1}S)n\ell n'\ell'$ double excitation region, respectively. The spectrum for each excitation region was measured in a separate run and normalized in the ordinate so that we can compare the relative excitation cross sections for these three excitation regions. As we can recognize from this figure, the photoexcitation cross sections for the deeply bound $[1s2s](^{3,1}S)n\ell n'\ell'$ series are extremely small. The series limits of the $[1s]\epsilon p$ and the $[1s2p](^{3,1}P)3p\epsilon p$ are indicated in the figure. Measured 2*p*-*np* shakeup energies [31,32] relative to the main Ne 1*s* line [33] have been adopted to estimate these $[1s2p](^{3,1}P)3p\epsilon p$ series limits. Furthermore, the 2*p*-ϵp shakeoff limits could also be estimated to be 916.87(11) eV for the $[1s2p](^{3}P)\epsilon p\epsilon' p$ and 921.47(11) eV for the $[1s2p](^{1}P)\epsilon p\epsilon' p$ doubly ionized states, respectively. Thus the $[1s2s](^{3,1}S)n\ell n'\ell'$ doubly excited states lie in the several continua stated above. The channels having the same symmetry can therefore interact and the discrete state included in this region becomes an autoionizing resonance which would have a Fano profile.

Figure 2 shows the normalized photoion yield spectrum in the region of the $[1s2s](^{3,1}S)n\ell n'\ell'$ doubly excited 2*p*-2*h* states of Ne plotted together with the results of theoretical calculations. We can see the pronounced peak at 924.8 eV, which corresponds to the $[1s2s](^{3}S)3s3p\ ^{1}P$ doubly excited 2*p*-2*h* state. The energy position of the series limit for the $[1s2s](^{3}S)3snp$ series could be estimated as 929.6 eV using the energy of the shakeup line observed in the x-ray photoemission spectrum [34].

The resonance energies and the oscillator strengths for the doubly excited 2*p*-2*h* states were calculated using a set of codes GRASP92 (General purpose Relativistic Atomic Structure Program 92) [35], which is an extension of the earlier version GRASP [36], CESD99 (a program for the Complete Expansion of *jj*-coupled symmetry functions into Slater Determinants) [37], and REOS99 (a program for Relaxed-orbital Oscillator Strength calculations) [38]. To obtain correctly the 1*s*2*s* double excitation energies and the dipole excitation functions, we have to evaluate properly (1) the contraction of the residual 1*s* and 2*s* electronic orbitals after the double electron excitations as well as the contraction of the 2*p*-subshell electronic orbitals after the 1*s*2*s* hole creation inside the 2*p* subshell, (2) the difference in magnitudes of 2*p* intrasubshell correlations for ground and doubly excited states of Ne atoms, and (3) the effect of correlations between the two electrons in the excited orbitals. The following procedure was devised for the present calculations. First, the Ne^{2+} $[1s2s](^{3,1}S)$ ionic states were calculated. We obtained a value $0.155a_0$ for the 1*s* orbital radius, where a_0 is the Bohr radius, and $0.79a_0$ for the 2*s* orbital radius, which are compared with the values $0.158a_0$ and $0.89a_0$ for the corresponding values of the ground state neutral Ne atoms. We can also compare the radii of the 2*p* orbital radius; those are $0.75a_0$ for Ne^{2+} and $0.96a_0$ for Ne. Second, we evaluated the 2*p* intrasubshell correlation energies. The total electronic energy of the ground state of Ne was lowered by 5.6 eV when we included all the possible 2*p* intrasubshell configurations such

as $2p^4 n\ell n'\ell'$ up to $n,n'=6$, whereas the corresponding energy lowering in the Ne^{2+} $[1s2s]({}^{3,1}S)$ was 6.2 eV. It is quite natural to consider the $2p$ intrasubshell correlation energies in the Ne $[1s2s]({}^{3,1}S)n\ell n'\ell'$ states will fall between those two values. Because the major part of this $2p$ intrasubshell correlation energies is canceled in the subtraction of the ground state energy from the excited state energy, in the actual calculation for the doubly excited states we neglected the $2p$ intrasubshell correlation effects; the resulting errors which we will encounter into the excitation energies are expected to be much less than $6.2-5.6=0.6$ eV. Finally, we calculated the energies and the oscillator strengths for the doubly excited states with $2p$-$2h$ configurations. All the possible two electron configurations with orbitals $3s$, $3p$, $3d$, and all the two electron configurations $3snp$ and $ns3p$ up to $n=6$ are included and the orbitals are optimized in the framework of MCDF approximations. The single electron orbitals are added and optimized in stepwise from the lower to higher lying orbitals. To obtain the minimal basis for the $[1s2s]({}^{3,1}S)3s3p$ states, we used the orbitals of the Ne^{2+} $[1s2s]({}^{3,1}S)$ states as initial vectors for $1s$, $2s$, and $2p$ orbitals. When we optimized the ns,np $(n\geqslant 4)$ orbitals, we fixed all the orbitals with the principal quantum numbers less than n.

Although the GRASP provides a means of calculating the oscillator strengths between the electronic states, this can be achieved when we use a unique orthonormal set of single electron orbital bases. In the present calculation, we have employed an alternative way to fit to the case of deep inner-shell multiple excitation. The single electron orbitals for the excited states were optimized separately from the ones for the ground states to fully take into account the orbital relaxation due to the electron escapes from inner shells. We obtained a pair of different orthonormal basis sets for excited and ground states, and they are not necessarily orthogonal. To calculate the oscillator strengths for the doubly excited states, the programs CESD99 [37] and REOS99 [38], which apply relativistic wave functions optimized by the GRASP92 package, were adopted to take into account properly the nonorthogonality of the bases between the initial and final states. Within the framework of Löwdin's formalism [39], the single-photon double-electron excitation can be described as the shake-up process induced by the inner-shell excitation, as was discussed in the previous work for shake-off process accompanying K-shell excitation in Ar [10].

As noted already, we show also the results of theoretical calculations in Fig. 2. The bar graph indicates the oscillator strengths for the $[1s2s]({}^{3,1}S)n\ell n'\ell'$ resonant double excitations calculated based on the velocity form transition dipole matrix elements. As we can see in this figure, the present calculations for series members of the $[1s2s]({}^{3,1}S)3snp$ $(3\leqslant n\leqslant 6)$ and the $[1s2s]({}^{3}S)3pns$ $(4\leqslant n\leqslant 6)$ doubly excited $2p$-$2h$ states have successfully reproduced the observed spectrum. Also the calculated series limits for the $[1s2s]({}^{3}S)3snp$ series, i.e., 928.77 eV for $J_f=3/2$ and 929.64 eV for $J_f=1/2$, reproduce the experimental results of 929.6 eV reasonably well, where J_f stands for the total angular momentum of final ionic states. The other calculated series limits are summarized in Table I. When we compare the calculated series limit of 937.2 eV for the $[1s2s]({}^{1}S)3snp$ series with the value of 936 eV estimated using the experimental results [31,33], we can reconfirm that the accuracy of the present calculations is satisfactory. With the aid of the good accuracy of the calculations, we have assigned the observed features as the energy markers for each series indicated in the upper part of Fig. 2. Calculated energy levels for these series members, which have oscillator strengths larger than 5×10^{-6}, as well as their characteristics, are summarized in Table II. We determined the energy positions for only the well-isolated double excitation resonance from the present measurement because of the poor statistics in the absorption spectrum.

TABLE I. Calculated energies of the series limits lie in the $[1s2s]({}^{3,1}S)n\ell n'\ell'$ double excitation region.

Final state configuration	J_f^π	Energy (eV)
$[1s2s]({}^3S)3s\epsilon p$	$3/2^+$	928.77
	$1/2^+$	929.64
$[1s2s]({}^3S)3p\epsilon s$	$1/2^-$	932.30
	$3/2^-$	932.31
	$5/2^-$	932.31
	$3/2^-$	932.62
	$1/2^-$	932.62
$[1s2s]({}^1S)3s\epsilon p$	$1/2^+$	937.24
$[1s2s]({}^1S)3p\epsilon s$	$1/2^-$	940.58
	$3/2^-$	940.59
$[1s2s]({}^3S)\epsilon s\epsilon' p$	1^+	942.54
$[1s2s]({}^1S)\epsilon s\epsilon' p$	0^+	950.74

Figure 3 represents the photoion yield spectrum of Ne in the region of the $[1s2s]({}^3S)3s3p$ resonant double excitation plotted together with a line shape fit. We used the well-known parametrized equations describing a single resonance line interacting with a continuum [40] given by

$$\sigma = \sigma_0\{\rho^2(q+\epsilon)^2/(1+\epsilon^2)+1-\rho^2\},$$

$$\epsilon = 2(E-E_0)/\Gamma,$$

$$\rho^2 = \sigma_a/(\sigma_a+\sigma_b),$$

where $\sigma_0=\sigma_a+\sigma_b$, σ_a is the portion of the continuum cross section which interacts with the resonance, E_0 is the resonance energy, Γ is the width of the resonance, and q and ρ^2 are the so-called Fano parameters that give the shape of the resonance and the strength of the continuum, respectively. We have carefully performed the Fano profile fit by means of a least-squares fitting procedure. We have convoluted the narrow bandpass ($\sim$121 meV) of the monochromator in the fitting procedure. The final fit to the experimental data yielded values $E_0=924.78\pm 0.12$ eV, $\Gamma=0.36\pm 0.02$ eV, $q=5.40\pm 0.58$, and $\rho^2=(1.06\pm 0.30)\times 10^{-3}$, respectively. Here we should note that the obtained width of the resonance, 0.36(02) eV, is significantly large as compared with those of the Ne $[1s]3p$ state [30] and the $[1s2p]({}^3P)3p^2$ resonant

TABLE II. Energy levels and oscillator strengths for the $[1s2s](^{3,1}S)n\ell n'\ell'$ resonant double excitation.

Energy (eV) Measured	Energy (eV) Calculated	Oscillator strength (units of 10^{-4})	Fractions of major configuration state functions (%) $(^3S):[1s2s](^3S)$, $(^1S):[1s2s](^1S)$
924.78 ± 0.12[a]	924.86	2.423	98.39 of $(^3S)3s3p+0.95$ of $(^3S)3p3d$
928.10 ± 0.12[b]	928.13	0.427	98.45 of $(^3S)3s4p+0.42$ of $(^3S)3p4s+0.22$ of $(^3S)3s3p$
	928.90	0.174	99.41 of $(^3S)3s5p+0.20$ of $(^3S)3p4s$
	929.23	0.080	99.68 of $(^3S)3s6p+0.11$ of $(^3S)3p4s$
930.71 ± 0.12[b]	930.57	0.237	96.06 of $(^3S)3p4s+1.26$ of $(^3S)3p3d$
	931.68	0.109	99.39 of $(^3S)3p5s+0.12$ of $(^3S)3p3d$
	932.12	0.053	69.46 of $(^3S)3p6s+30.44$ of $(^3S)3p5s+0.01$ of $(^3S)3s6p$
	934.57	0.466	72.33 of $(^1S)3s3p+17.56$ of $(^1S)3s4p+4.07$ of $(^1S)3p3d$
	936.15	0.214	74.07 of $(^1S)3s4p+11.03$ of $(^1S)3s3p+6.19$ of $(^1S)3s5p$
	936.71	0.110	83.77 of $(^1S)3s5p+3.16$ of $(^1S)3s6p+2.71$ of $(^1S)3s3p$
	936.99	0.061	91.68 of $(^1S)3s6p+1.80$ of $(^1S)3p4s+1.34$ of $(^1S)3s5p$
	938.90	0.250	88.21 of $(^1S)3p4s+4.15$ of $(^1S)3s4p+1.79$ of $(^1S)3p5s$
	939.76	0.118	93.24 of $(^1S)3p5s+2.28$ of $(^1S)3p3d+0.79$ of $(^1S)3p4s$
	940.14	0.072	86.99 of $(^1S)3p6s+10.37$ of $(^1S)3p3d+0.95$ of $(^1S)3s3p$

[a]Resonance energy determined by Fano profile fitting.
[b]Peak position determined by the fitting procedure using Gaussian profile.

double excitation [14]. As we have stated before, the $[1s2s](^3S)3s3p$ double excitation resonance lies in the several continua, thus the interaction with those continua might have a significant effect of making the width of the resonance larger. This is in line with the explanation for the large width of the autoionizing resonance observed in the core-electron shakeup spectrum of Ne [34].

In order to interpret the line profile of the $[1s2s](^3S)3s3p$ double excitation resonance, it is interesting to discuss decay channels for this $2p$-$2h$ state. From the analogy of the decay channels following the $[1s2p](^{3,1}P)3p^2$ resonant double excitation [14], the contribution of double-spectator type Auger transitions would be the dominant process. In order to confirm this situation, we have calculated the transition rates for the available resonant Auger processes based on the Hartree-Fock (HF) approximation using Cowan's code [15]. Auger transition produces

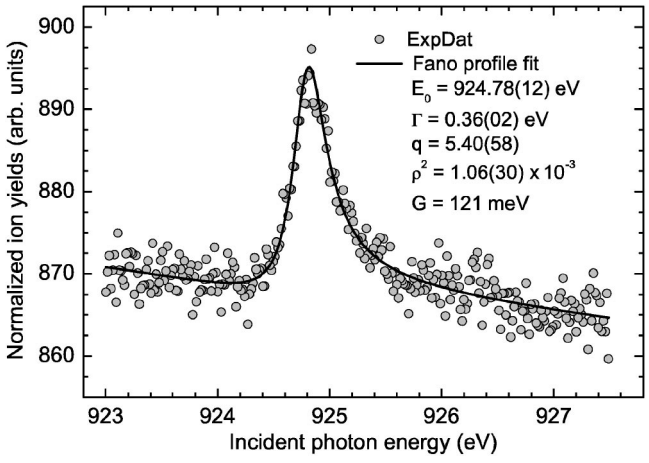

FIG. 3. Resonance of the $[1s2s](^3S)3s3p$ doubly excited $2p$-$2h$ state plotted together with a Fano profile fitting.

many final ionic states, and the typical decay channels are given by

$$
\begin{aligned}
[1s2s](^3S)3s3p &\rightarrow [2s2p^2]3s3p + e^- \text{ (a)} \\
&\rightarrow [2s^2 2p]3s3p + e^- \text{ (b)} \\
&\rightarrow [2s2p]3s + e^- \text{ (c)} \\
&\rightarrow [2s2p]3p + e^- \text{ (d)} \\
&\rightarrow [2s] + e^- \text{ (e)}.
\end{aligned}
$$

Here (a) and (b) are the double-spectator, (c) and (d) the spectator-participator, and (e) the double-participator type transitions, respectively. Some of these final states proceed further via a second-step process. Furthermore, there should be a number of more complicated shake-modified decay channels that associate the channels (a)–(d), but these are expected to be with only minor contributions to the whole decay paths. Thus we have omitted those channels from the present calculations. According to our simple estimation based on the HF approximation, the process (a) would be the leading term for the decay channels, e.g., about 78% of the branching ratio among the processes (a)–(e).

It is noteworthy, however, that the so-called inner-valence Auger transitions such as $[1s2s](^3S)3s3p \rightarrow [1s2p]3\ell + e^-$, which are similar to the usual Coster-Kronig transitions, are allowed. According to our calculations, these transitions make a significant contribution of about 50% relative to the process (a) and the final ionic states may have the same symmetries as the shakeup continua produced via direct ionization channels. Although both of these $[1s2p]3\ell$ ionic states, which are produced by direct and indirect channels, proceed further via an Auger decay, the interference between these two channels may be accountable for giving rise to the Fano profile.

IV. CONCLUSION

We have studied the photoabsorption spectrum of Ne in the region of the $[1s2s](^{3,1}S)3snp$ $(3 \leqslant n \leqslant 6)$ as well as the $[1s2s](^3S)3pns$ $(4 \leqslant n \leqslant 6)$ resonant double excitation. The observed absorption spectrum was analyzed with the aid of the theoretical calculations based on the MCDF method. The observed features were successfully assigned by comparing with the theoretical energies and the oscillator strengths. The spectral shape leading to the lowest resonance of the $[1s2s](^3S)3s3p$ state has been discussed in terms of the well-known parametrized Fano profile. The energy as well as the width of the resonance for such highly correlated multiply excited $2p$-$2h$ state have been determined and the possible decay channels for the $[1s2s](^3S)3s3p$ state were also discussed.

ACKNOWLEDGMENTS

We are grateful to Dr. S. Shin of RIKEN for his understanding during the accomplishment of this experiment at BL17SU. We thank Dr. K. C. Prince for making his results available prior to publication.

[1] R. D. Deslattes, R. E. LaVilla, P. L. Cowan, and A. Henins, Phys. Rev. A **27**, 923 (1983).
[2] J. M. Esteva, B. Gauthé, P. Dhez, and R. C. Karnatak, J. Phys. B **16**, L263 (1983).
[3] M. Deutsch and M. Hart, Phys. Rev. Lett. **57**, 1566 (1986).
[4] S. Bodeur, P. Millié, E. Lizou à Lugrin, I. Nenner, A. Filipponi, F. Boscherini, and S. Mobilio, Phys. Rev. A **39**, 5075 (1989).
[5] U. Kuetgens and J. Hormes, Phys. Rev. A **44**, 264 (1991).
[6] M. Štuhec, A. Kodre, M. Hribar, D. Glavič-Cindro, I. Arčon, and W. Drube, Phys. Rev. A **49**, 3104 (1994).
[7] C. Reynaud, M.-A. Gaveau, K. Bisson, P. Millié, I. Nenner, S. Bodeur, P. Archirel, and B. Lévy, J. Phys. B **29**, 5403 (1996).
[8] L. Avaldi, R. Camilloni, G. Stefani, C. Comicioli, M. Zacchigna, K. C. Prince, M. Zitnik, C. Quaresima, C. Ottaviani, C. Crotti, and P. Perfetti, J. Phys. B **29**, L737 (1996).
[9] M. Oura, T. Mukoyama, M. Taguchi, T. Tekauchi, T. Haruna, and S. Shin, Phys. Rev. Lett. **90**, 173002 (2003).
[10] J. W. Cooper, Phys. Rev. A **38**, 3417 (1988).
[11] H. P. Saha, Phys. Rev. A **42**, 6507 (1990).
[12] Y. Azuma, S. Hasegawa, F. Koike, G. Kutluk, T. Nagata, E. Shigemasa, A. Yagishita, and I. A. Sellin, Phys. Rev. Lett. **74**, 3768 (1995).
[13] Y. Azuma, F. Koike, J. W. Cooper, T. Nagata, G. Kutluk, E. Shigemasa, R. Wehlitz, and I. A. Sellin, Phys. Rev. Lett. **79**, 2419 (1997).
[14] M. Oura, Y. Tamenori, T. Hayaishi, Y. Kanai, H. Yoshii, K. Tsukamoto, and F. Koike, Phys. Rev. A **70**, 022710 (2004).
[15] R. D. Cowan, *The Theory of Atomic Structure and Spectra* (University of California Presss, Berkeley, 1981).
[16] N. M. Kabachnik and I. P. Sazhina, J. Phys. B **17**, 1335 (1984); N. M. Kabachnik (private communication).
[17] M. Oura, M. Machida, and Y. Tamenori, in Program and Abstracts of the 14th International Conference on Vacuum Ultraviolet Radiation Physics (VUV-14), Cairns, Australia, 2004 (unpublished), p. 211; M. Oura *et al.* (unpublished).
[18] T. Åberg, Proceedings of a Workshop held at Argonne National Laboratory, Atomic Physics at High Brilliance Synchrotron Sources, ANL/APS/TM-14, 1994 (unpublished), p. 167.
[19] G. B. Armen, H. Aksela, T. Åberg, and S. Aksela, J. Phys. B **33**, R49 (2000).
[20] K. C. Prince, R. Sankari, L. Avaldi, R. Richter, M. de Simone, and M. Coreno, in Program and Abstracts of the 14th International Conference on Vacuum Ultraviolet Radiation Physics (VUV-14), Cairns, Australia, 2004 (unpublished), p. 74; K. C. Prince *et al.* (unpublished).
[21] M. Oura, T. M. Kojima, Y. Awaya, Y. Itoh, K. Kawatsura, M. Kimura, T. Koizumi, T. Sekioka, H. Yamaoka, and M. Cox, J. Synchrotron Radiat. **5**, 1058 (1998).
[22] M. Oura, H. Yamaoka, K. Kawatsura, T. Hayaishi, J. Kimata, T. M. Kojima, M. Kimura, T. Sekioka, and M. Terasawa, Rev. Sci. Instrum. **71**, 1206 (2000).
[23] See, for example, http://www.spring8.or.jp/e/publication/blhb/bl17su.pdf
[24] K. Shirasawa, T. Tanaka, T. Seike, A. Hiraya, and H. Kitamura, in *Proceedings of the 8th International Conference on Synchrotron Radiation Instrumentation*, AIP Conf. Proc. No. 705 (AIP, Melville, NY, 2003), p. 203.
[25] H. Ohashi, Y. Senba, H. Kishimoto, T. Miura, S. Takahashi, H. Aoyagi, M. Sano, Y. Furukawa, T. Nakatani, T. Ohata, T. Matsushita, Y. Ishizawa, S. Taniguchi, Y. Asano, K. Takeshita, S. Goto, E. Ishiguro, M. Oura, and S. Shin (unpublished).
[26] M. Oura, H. Yamaoka, K. Kawatsura, J. Kimata, T. Hayaishi, T. Takahashi, T. Koizumi, T. Sekioka, M. Terasawa, Y. Itoh, Y. Awaya, A. Yokoya, A. Agui, A. Yoshigoe, and Y. Saitoh, Phys. Rev. A **63**, 014704 (2001).
[27] H. Yamaoka, M. Oura, K. Kawatsura, T. Hayaishi, T. Sekioka, A. Agui, A. Yoshigoe, and F. Koike, Phys. Rev. A **65**, 012709 (2002).
[28] K. Kawatsura, H. Yamaoka, M. Oura, T. Hayaishi, T. Sekioka, A. Agui, A. Yoshigoe, and F. Koike, J. Phys. B **35**, 4147 (2002).
[29] K. W. Jones, B. M. Johnson, and M. Meron, Phys. Lett. **97A**, 377 (1983).
[30] A. De Fanis, N. Saito, H. Yoshida, Y. Senba, Y. Tamenori, H. Ohashi, H. Tanaka, and K. Ueda, Phys. Rev. Lett. **89**, 243001 (2002).
[31] S. Svensson, B. Eriksson, N. Mårtensson, G. Wendin, and U. Gelius, J. Electron Spectrosc. Relat. Phenom. **47**, 327 (1988).
[32] N. Mårtensson, S. Svensson, and U. Gelius, J. Phys. B **20**, 6243 (1987).
[33] L. Avaldi, G. Dawber, R. Camilloni, G. C. King, M. Roper, M. R. F. Siggel, G. Stefani, M. Zitnik, A. Lisini, and P. Decleva, Phys. Rev. A **51**, 5025 (1995).
[34] S. Svensson, N. Mårtensson, and U. Gelius, Phys. Rev. Lett. **58**, 2639 (1987).

[35] F. A. Parpia, C. F. Fischer, and I. P. Grant, Comput. Phys. Commun. **94**, 249 (1996).
[36] K. G. Dyall, I. P. Grant, C. T. Johnson, F. A. Parpia, and E. P. Plummer, Comput. Phys. Commun. **55**, 425 (1989).
[37] S. Fritzsche and J. Anton, Comput. Phys. Commun. **124**, 353 (2000).
[38] S. Fritzsche, C. F. Fischer, and C. Z. Dong, Comput. Phys. Commun. **124**, 340 (2000).
[39] P. O. Löwdin, Phys. Rev. **97**, 1474 (1955).
[40] U. Fano and J. W. Cooper, Phys. Rev. **137**, A1364 (1965).